ADVANCES IN ATMOSPHERIC SCIENCES, VOL. 25, NO. 6, 2008, 1062–1072

The Effect of Typhoon-Induced SST Cooling on Typhoon Intensity: The Case of Typhoon Chanchu (2006)

JIANG Xiaoping[1,2] (蒋小平), ZHONG Zhong[*1] (钟 中), and LIU Chunxia[2,3] (刘春霞)

[1] *Institute of Meteorology, PLA University of Science and Technology, Nanjing* 211101

[2] *Guangzhou Institute of Tropical and Marine Meteorology, China Meteorological Administration, Guangzhou* 510080

[3] *Key Laboratory of Tropical Marine Environmental Dynamics, South China Sea Institute of Oceanology, Chinese Academy of Sciences, Guangzhou* 510301

(Received 28 September 2007; revised 7 January 2008)

ABSTRACT

In order to investigate air-sea interactions during the life cycle of typhoons and the quantificational effects of typhoon-induced SST cooling on typhoon intensity, a mesoscale coupled air-sea model is developed based on the non-hydrostatic mesoscale model MM5 and the regional ocean model POM, which is used to simulate the life cycle of Typhoon Chanchu (2006) from a tropical depression to a typhoon followed by a steady weakening. The results show that improved intensity prediction is achieved after considering typhoon-induced SST cooling; the trend of the typhoon intensity change simulated by the coupled model is consistent with observations. The weakening stage of Typhoon Chanchu from 1200 UTC 15 May to 1800 UTC 16 May can be well reproduced, and it is the typhoon-induced SST cooling that makes Chanchu weaken during this period. Analysis reveals that the typhoon-induced SST cooling reduces the sensible and latent heat fluxes from the ocean to the typhoon's vortex, especially in the inner-core region. In this study, the average total heat flux in the inner-core region of the typhoon decrease by 57.2%, whereas typhoon intensity weakens by 46%. It is shown that incorporation of the typhoon-induced cooling, with an average value of 2.17°C, causes a 46-hPa weakening of the typhoon, which is about 20 hPa per 1°C change in SST.

Key words: coupled model, air-sea interaction, typhoon intensity, SST cooling

Citation: Jiang, X. P., Z. Zhong, and C. X. Liu, 2008: The effect of typhoon-induced SST cooling on typhoon intensity: The case of Typhoon Chanchu (2006). *Adv. Atmos. Sci.*, **25**(5), 1062–1072, doi: 10.1007/s00376-008-1062-9.

1. Introduction

The typhoon is accompanied by the most intense air-sea interactions on a synoptic scale. When a typhoon propagates over the ocean surface, the surface wind stress generates ocean currents and strong turbulent mixing in the ocean. The mixing deepens the ocean mixed layer, entraining cooler thermocline water into it, which lowers the SST (Price, 1981; Price et al., 1994; Shay et al., 2000; Sheng et al., 2006). Observational studies have shown that the maximum SST cooling can reach up to 9°C (Sakaida et al., 1998). On the other hand, the SST cooling reduces the sea surface heat fluxes, which subsequently leads to reduced typhoon intensity (Sutyrin and Khain, 1984; Khain and Ginis, 1991; Falkovich et al., 1995).

Due to the lack of observational data over the oceans, the main method used to research the effect of SST cooling on typhoon intensity is dependent on the coupled air-sea model. The earliest simulations of the coupled air-sea model were performed by Elsberry et al. (1976), Chang and Anthes (1978) and Sutyrin and Khain (1979) with a coarse resolution. Their calculations suggested that the effects of SST cooling on typhoon intensity are small. There may be some limitations of using an axisymmetric typhoon model as

*Corresponding author: ZHONG Zhong, zhongzhong@jsmail.com.cn

part of a coupled model, especially on the scale of the inner core, because the ocean response is asymmetric about the moving typhoon center (Zhu et al., 2004). Presently, three-dimensional hurricane-ocean coupled models have been used in studies with a relatively high resolution (Schade and Emanuel, 1999; Bender and Ginis, 2000; Huang et al., 2005). Results have shown that typhoon-induced SST cooling can weaken typhoon intensity significantly. Improved intensity prediction was achieved to a great extent after considering typhoon-induced SST cooling. Bender and Ginis (2000) preformed several real-data simulations with the Geophysical Fluid Dynamics Laboratory (GFDL) hurricane model coupled with the Princeton Ocean Model (POM). The errors of the hurricane intensity simulated by their coupled model were generally weaker than those without using a coupled model.

While the previous studies generally agree that typhoon-induced SST cooling can have a significant impact on the typhoon intensity, they disagree concerning the quantitative relationship between the typhoon-induced SST cooling and the weakening of the typhoon. In the study of Ren and Perrie (2006), the typhoon was weakened by 7 hPa per 1.0°C decrease in SST, which was close to the rate of 10 hPa $^{\circ}C^{-1}$, the result that Emanuel (1991) obtained under a typical typhoon environment based on the Carnot engine concept. However, in the study of Holland (1997), the quantitative relationship, which was obtained using a thermodynamic approach, was 33 hPa $^{\circ}C^{-1}$. According to Zhu and Zhang (2006), a change in SST by 1°C results in the weakening of typhoon intensity by 20 hPa, which was relatively close to the rate of 16 hPa $^{\circ}C^{-1}$, as suggested by Chan et al. (2001) using a coupled model. Chan et al. (2001) pointed out that the quantitative relationship in Emanuel's study was underestimated because thermodynamic processes within much of the troposphere had not been considered, and in Holland's study, dissipation mechanisms were ignored, so his quantitative relationship was overestimated.

Recent studies showed that the weakening of typhoon intensity mainly results from the SST cooling within the inner-core region of the typhoon, although the largest SST decrease occurs in the right-rear quadrant. According to Weatherford and Gray (1988), the "inner core" of a typhoon is defined to extend from the center out to a 111-km radius. Cione and Uhlhorn (2003) studied the correlation of SST change and changes in typhoon intensity using airborne expendable bathythermograph (AXBT) observations and buoy-derived archived SST data. They used this to highlight the significant impacts of the changes in inner core SST on the magnitude of air-sea fluxes within the high-wind inner core region. Relatively modest changes in inner core SST could effectively alter maximum total heat flux. Zhu and Zhang (2006) performed a simulation of Hurricane Bonnie (1998) with the MM5 model. The SST field was updated daily using the Tropical Rainfall Measuring Mission (TRMM) Microwave Imager (TMI) level 1 standard product at $0.25^{\circ} \times 0.25^{\circ}$ latitude-longitude resolution to represent the typhoon-induced SST changes. Two additional sensitivity simulations were performed in which the typhoon-induced cooling was either ignored or shifted towards the modeled storm track. Results showed marked sensitivity of the model-simulated storm intensity to the magnitude and relative position with respect to the hurricane track. In the absence of the SST cooling, the model produced the strongest hurricane, whereas shifting the SST cooling close to the storm track generated the weakest storm. Zhu et al. (2004) investigated the interaction between a tropical cyclone and the ocean using a three-dimensional tropical cyclone model coupled with a two-layer ocean model. Two representations for entrainment into the ocean mixed layer were compared: one based on the turbulent erosion model (TEM) and the other based on the dynamic instability model (DIM). Although the experiment based on the TEM produced a much smaller maximum SST cooling because the cooling was directly underneath the hurricane core, it was more effective in reducing the heat flux from the ocean to the storm in the inner-core region and led to a greater reduction of the tropical cyclone intensity.

The purposes of the present study are to investigate the air-sea interactions during the life cycle of the typhoon and to quantify the impact of the typhoon-induced SST cooling on typhoon intensity. We couple the non-hydrostatic mesoscale model MM5 and the regional ocean model POM and then simulate the evolution of Typhoon Chanchu (2006) from a very weak tropical depression into a typhoon followed by a steady weakening. In this way we investigate the air-sea interactions during the life cycle of Typhoon Chanchu. A brief description of the coupled model used in this study is presented in section 2. The typhoon case and the experimental design are also described there. Numerical results of the typhoon simulations are discussed in section 3, while the impact of SST cooling on the typhoon is analyzed in section 4. Summary and conclusions are intensity given in section 5.

2. The coupled model

2.1 *Experimental design*

In this paper, Typhoon Chanchu, which occurred

in the South China Sea (SCS) in 2006, is taken as an example to conduct the simulation experiment (hereafter referred to as CEX). Chanchu formed at 1200 UTC 9 May 2006 over the sea east of the Philippines. It moved northwestward steadily after its generation and strengthened gradually. At 0000 UTC 13 May it strengthened to a typhoon in the SCS. Thereafter, Chanchu moved westward slowly with a moving speed range of 2.7–4.2 m s^{-1} and then suddenly turned northward at 0000 UTC 15 May. Chanchu moved rapidly and made landfall in the coastal area between Chenhai and Raopin, in Guangdong Province in China at 1815 UTC 17 May. Chanchu was the first typhoon to make landfall in China in 2006. Its landing time was 44 days earlier than the climatological average. It was the earliest typhoon to hit Guangdong Province and also one of the most intense typhoons to make landfall in China in May since 1949.

In this study, POM is taken as the ocean part of the coupled model (Bao et al., 2004). As shown in Fig. 1, POM is implemented on the domain of 0°N to 30°N and 99°E to 130°E, covering all of the SCS and the western portion of the Pacific. A uniform horizontal resolution of $0.25° \times 0.25°$ is used. In the vertical, there are 21 sigma layers with finer resolution in the upper ocean. The external time step is taken to be 60 s and internal time step 1800 s. The western boundary is fixed and the other three boundaries open. Monthly velocity, elevation, salinity and temperature fields from the Simple Ocean Data Assimilation (SODA) have been interpolated to model grids as dynamic forcing at the open boundaries, with the in- and out-flux being balanced. Gravity wave radiation condition is applied to the velocity component perpendicular to the open boundaries. An upwind-advection scheme is applied to temperature, salinity, and the velocity component parallel to the boundary so that in the case of inflow the boundary conditions derived from the SODA data are imported by inward velocities. MM5 is used as the atmospheric part of the coupled model, with two-nested domains. The outer domain D01 has 181×151 grid points, with 15 km grid spacing in the horizontal and 32 layers in the vertical; the time step is set to 50 s. No bogus scheme is used. The initial conditions and lateral boundary conditions come from the NCEP analysis data with $1° \times 1°$ resolution. MM5 is integrated for 126 h, from 0600 UTC 12 May to 1200 UTC 17 May 2006. This 126-h integration covers several important periods in the life cycle of Typhoon Chanchu, including its formation, rapid intensification, propagation westward in the SCS, its abrupt northward movement and decay stage. The air-sea coupling occurs over the limited-area D01 domain. The inner domain D02 has 181×241 grid points. A one-way nested grid is used with 5 km grid spacing in the horizontal and 32 layers in the vertical. The time step is set to 18 s. The initial and boundary conditions in the D02 simulation are provided by hourly output from the D01 simulation. It is initialized at 1300 UTC 14 May and is integrated for 48 h, covering the time period when Chanchu developed into its strongest stage after turning northward and then weakening gradually in its decay stage. MM5's model physics include the Betts-Miller cumulus parameterization scheme (implicit) and the Reisner II (explicit) microphysics scheme. Besides these physics process schemes, the shallow convection scheme and the MRF planetary boundary layer scheme are utilized, with the radiation scheme taken from CCM2 (Climate Community Model version 2).

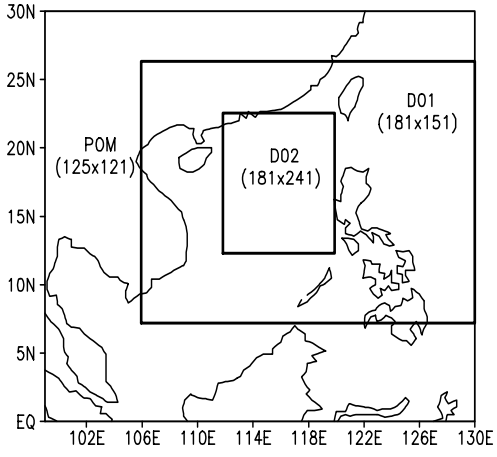

Fig. 1. Domain configuration for CEX, D01 and D02 denotes twi-nested MM5 simulation domain respectively and the outer domain is for POM simulation. Dimensions of each domain (north-south by east-west) are shown.

To examine the improvement in typhoon simulation after typhoon-induced SST cooling is taken into account, we conducted another simulation using MM5 with no coupling with POM. SST values at 0600 12 May 2006 from ocean model initialization are used and they are not varied during the integration. This simulation is denoted as the uncoupled experiment (hereafter referred to as UEX).

2.2 *The method of coupling*

After POM initialization, during the period of one POM internal time step, MM5 is integrated using the SST field from POM initialization. The surface wind speed, latent heat fluxes and sensible heat fluxes computed in the MM5 model are passed on to POM. POM is then integrated over one internal step and a new SST field is calculated. The new SST field is used in the ensuing time steps of MM5. Due to different model

meshes used in MM5 and POM, the transfer of the surface wind speed, heat fluxes from MM5 to POM, as well as the transfer of the SST field from POM to MM5, are all accomplished through interpolation. In this way, MM5 is driven using variations in SST simulated by POM, and POM is forced using the surface wind speed and heat fluxes from MM5, which reflect a realistic simulation of the typhoon and ocean.

2.3 *Ocean model initialization*

The importance of a realistic ocean initialization for proper simulation of the ocean response in the coupled typhoon-ocean model can not be overemphasized (Bender and Ginis, 2000). In this study the initialization procedure included three steps. First, POM was integrated from the calm state of ocean. The initial temperature and salinity were provided by the Levitus dataset for January, and the wind stress was obtained from COADS. They were both horizontally and vertically interpolated to each grid on each of the 21 sigma-layers. After 2 model years, the model reached a quasi-equilibrium state (Zhang and Qian, 1999). This was followed by a second procedure to adjust the upper ocean structure to a more realistic pre-storm condition at the start of typhoon forecast. During this integration, POM was forced by the wind stress from the NCEP reanalysis data, net heat fluxes, and shortwave radiation from the Southampton Oceanography Centre (SOC). In the third procedure, the daily-averaged SST on 12 May 2006 was obtained from TRMM/TMI and assimilated into the model (Bender and Ginis, 2000). The assimilation procedure involved the replacement of the SST field in the upper ocean mixed layer with the TRMM/TMI SST field and prognostic model integration for another 10 days for dynamical adjustment. During this integration, the SST field at the surface was kept constant.

3. Experimental results

3.1 *Overview of the simulated typhoon results*

It is evident from Fig. 2 that the simulated track in CEX is similar to that in UEX (in this paper we assume that unless mentioned otherwise, results are all from the D01 simulation), and both follow the observed track closely. Thus, we may state that the typhoon track is not sensitive to the typhoon-induced SST cooling, as shown in previous studies (e.g., Zhu et al., 2004; Zhu and Zhang, 2006). A comparison of the simulated and observed tracks reveal a reasonably accurate simulation, especially considering that there is no bogusing of the storm to match the initial conditions and that there is no continuous data assimilation as the simulation progresses. The tracks in CEX and

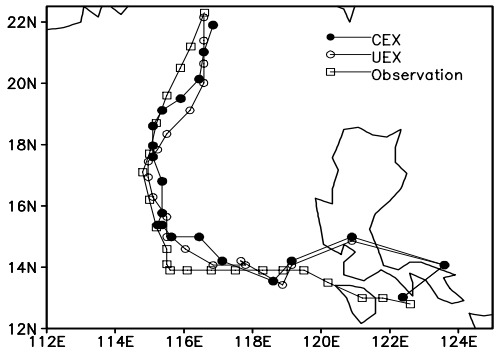

Fig. 2. The simulated and observed tracks of Chanchu (shaded circles: CEX, open circles: UEX, open rectangles: observation).

UEX appear to agree less with observations early in the development from 0600 UTC 12 May to 0600 UTC 13 May. Part of the error is due to the fact that the low-level cyclonic circulation is broad and weak, as shown in some simulations (e.g., Davis and Bosart, 2001).

The simulated minimum surface pressure values in CEX are consistently better in comparison with observations than those of UEX, for both D01 and D02 (see Fig. 3). In CEX, the simulated typhoon intensity reproduces Chanchu's rapid deepening stage, the maintaining stage, and the steady weakening stage very well. Chanchu continued to intensify from 0600 UTC 12 May to 0000 UTC 15 May, with the central pressure dropping from 984 hPa to 948 hPa. Thereafter Chanchu maintained its intensity until 1200 UTC 15, and then began to weaken steadily. The central pressure was 969 hPa at 1200 UTC 17 May. The D01 simulated typhoon in CEX deepens rapidly from 0600 UTC 12 May and reaches its minimum central pressure of 949 hPa at 0000 UTC 15 May, which is very close to the observation (948 hPa). The simulated typhoon weakens steadily from 0600 UTC 15 May and then strengthens a little after 0000 UTC 17 May. By comparison, UEX produces a much stronger typhoon than CEX. The simulated typhoon in UEX deepens excessively from 0600 UTC 12 May to 1800 UTC 16 May. Its peak central pressure is 903 hPa, 46 hPa lower than the observation. It fails to reproduce the typhoon weakening stage from 1200 UTC 15 May to 1800 UTC 16 May because SST is invariant without considering typhoon-induced SST cooling. However, it is the typhoon-induced SST cooling that makes Typhoon Chanchu weaken during this period.

3.2 *The SST cooling induced by Typhoon Chanchu*

Figure 4a shows the difference of daily-averaged

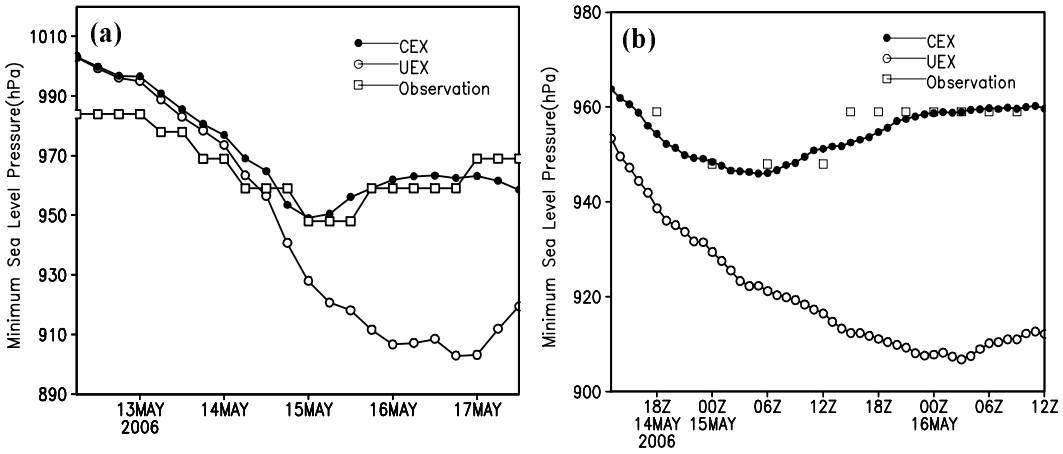

Fig. 3. Time series of minimum sea level pressure in hPa for CEX (shaded circles), UEX (open circles) and observation (open rectangles). Here (a), (b) are for D01 and D02 simulations, respectively.

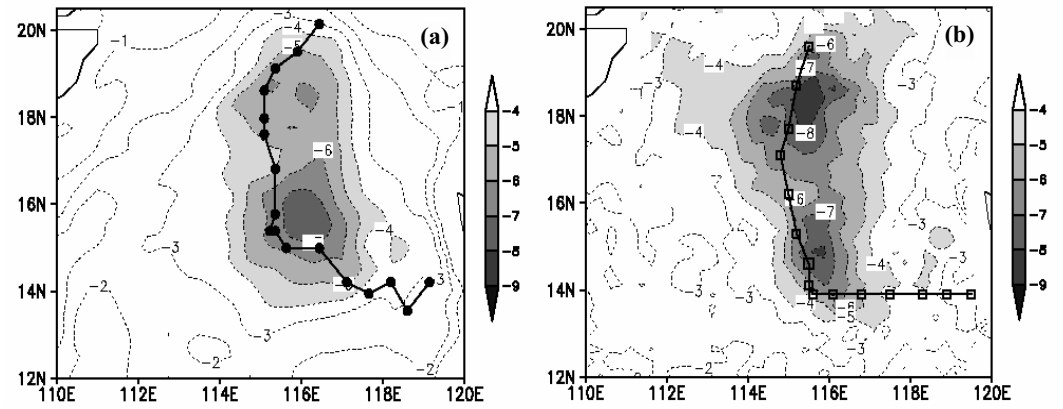

Fig. 4. (a) The simulated daily-averaged SST difference between 17 May and 12 May and (b) TRMM/TMI observed SST difference during the same period. There are some missing data in TRMM/TMI observed SST field. The shaded circles in (a) represent the typhoon track simulated by CEX, and the open rectangles in (b) represent the observed track.

SST between 17 May and 12 May simulated by POM in CEX. When compared with the difference of TRMM/TMI-derived daily-averaged SST during the same period (Fig. 4b), it is evident that the simulated SST cooling is consistent with observation. During this period, the relatively slow movement of Chanchu causes very large SST cooling in the SCS, with a pronounced rightward bias in the SST cooling with respect to the typhoon track. The extent of the region with SST cooling larger than 2°C is at least 10.0×10^5 km^2, a very large area. The maximum SST cooling is 8.5°C, which matches the maximum TRMM/TMI-derived SST cooling of 8.3°C well. Chanchu produces two cold wakes with SST cooling larger than 6°C. One is around 116.0°E and 15.5°N, which is located north of the TRMM/TMI observed wake. This is because the simulated storm takes a more northward track than that observed during 21–33 h. The other cold wake is around 116.0°E and 18.5°N. These two cold wakes are about 65 km and 107 km to the right of the typhoon track, respectively.

The rightward bias in the SST cooling is well established from previous observations and numerical studies. Shay et al. (1992) investigated the evolving upper ocean response excited by the passage of hurricane Gilbert (1988). According to Shay et al. (1992), both the AVHRR (Advanced Very High Resolution Radiometer) images and the objectively analyzed fields indicated a rightward bias in the upper ocean cooling that extended from the storm track to about $4R_{\max}$ (where $R_{\max}$, the radius of maximum winds, was equal to 50 km). Wada (2005) used TRMM/TMI observed SST to analyze the SST cooling resulting from Typhoon Fex (1998), and found that the SST cooling was

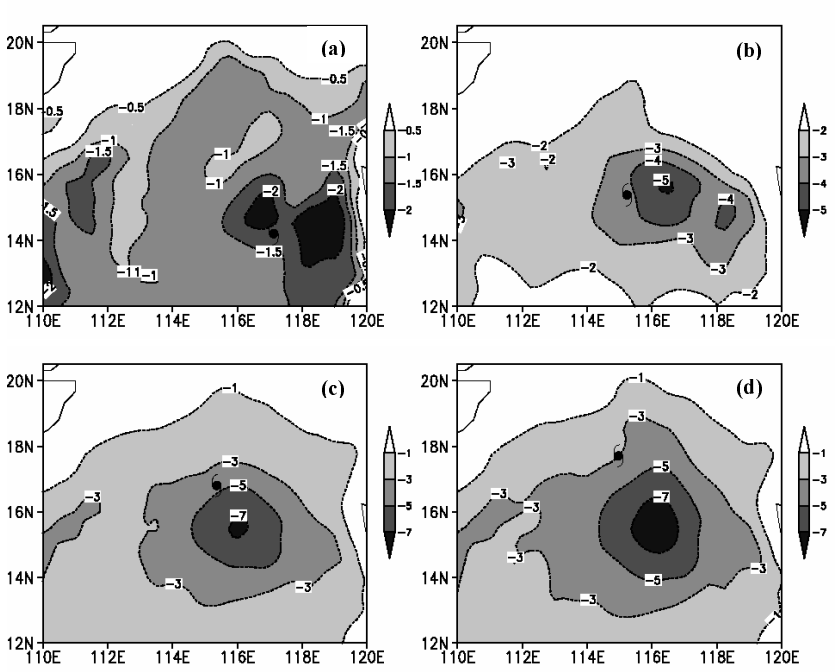

Fig. 5. Changes of the simulated SST at (a) 0000 UTC 14 May, (b) 0000 UTC 15 May, (c) 1200 UTC 15 May and (d) 0000 UTC 16 May in CEX. Here the typhoon center positions are shown by the typhoon symbols.

evident along the track and on the right side of the running typhoon.

Figure 5 shows the SST cooling induced by Chanchu in different life cycle stages. In the early integration when Chanchu is a tropical depression, its wind speeds are relatively low and it moves very quickly. The SST cooling is about 1°C in the central SCS, and there is no obvious SST cooling center formed (figure not provided). At 0000 UTC 14 May an SST cooling center is formed on the right side of the typhoon center with the maximum SST cooling of more than (Fig. 5a), about 130 km away from the typhoon center. At that time, the SST cooling within the inner-core region is about 1.5°C. Thereafter, the SST cooling becomes more and more obvious and the maximum SST cooling center gets nearer to the typhoon center due to the slow movement of Chanchu (merely 1.1 m s^{-1} at its slowest). At 0000 UTC 15, there is a great SST cooling area formed in the right-rear quadrant of the typhoon with SST cooling over 4.0°C (Fig. 5b). The maximum SST cooling center is around 116.0°E and 15.5°N, with the maximum SST cooling of 5°C, 84 km away from the typhoon center. At that time, the SST cooling within the inner-core region is over 4°C. Typhoon Chanchu is strongest from 0000 UTC 15 to 1200 UTC 15 May with a moving speed of 2.5–3.9 m s^{-1}, which is very favorable for SST cooling. By 1200 UTC 15 May, the SST drops further at the SST cooling center around 116.0°E and 15.5°N. The maximum SST cooling is more than 7°C. The SST cooling is generally over 6°C behind the typhoon and over 5°C within the inner-core region (Fig. 5c). The simulation of the SST cooling induced by Typhoon Fex performed by Wada (2005) also showed that SST cooling under the slowest translation stage is the greatest through the generation, development, and sustenance stages of Typhoon Rex. Thereafter, the position where the maximum SST cooling occurs hardly changes although the typhoon moves faster (Fig. 5d), which is consistent with other simulations (e.g., Wada, 2005). After 0000 UTC 17 May, there is another SST cooling center formed around 116.0°E and 18.2°N, with the largest SST decrease being 6°C. In conclusion, the ocean response is highly asymmetric about the moving typhoon center, especially on the scale of the inner core. SST cooling is obvious in the right-rear quadrant of the typhoon, whereas in the inner-core region the SST cooling is less than that in the right-rear quadrant.

4. Heat fluxes exchange between ocean and the vortex

Because of the significant intensity changes, the incorporation of the typhoon-induced cooling also causes pronounced structural changes in surface winds.

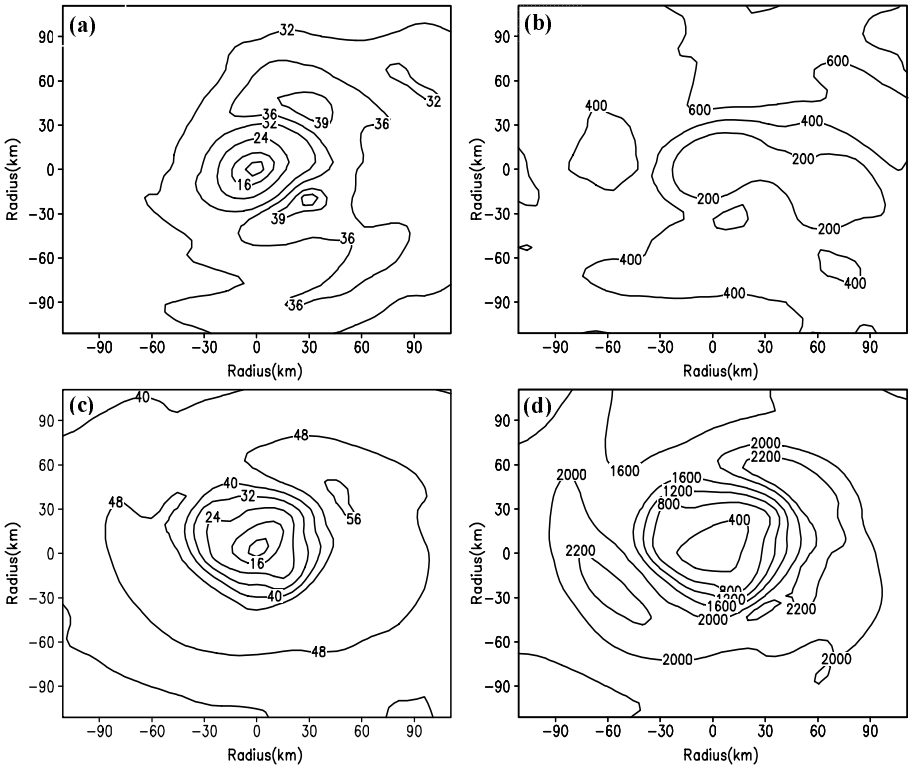

Fig. 6. (a, c) The simulated surface winds in m s^{-1} and (b, d) total heat fluxes in W m^{-2} in the inner-core region at 0900 UTC 15 May on D02 for (a, b) CEX and (c, d) UEX.

Figures. 6a, 6c show that the distribution of wind fields and the magnitude of wind speed in these two simulations differ from each other. UEX produces surface winds with the maximum wind speed of 56 m s^{-1}, much stronger than that in CEX, whose maximum wind speed is 41 m s^{-1}. Moreover, compared with UEX, CEX results show that there is a much more significant asymmetry in the distribution of the wind field around the typhoon center. Therefore, the SST cooling makes some contributions to the formation of the asymmetry in the wind field. As expected, the spatial structure of the total heat fluxes (sensible heat fluxes plus latent heat fluxes) in UEX is similar to the surface wind structure (see Fig. 6d). In the eye region, the underlying ocean provides much less surface flux to the typhoon due to low wind speeds. Surrounding the eye, large quantities of surface heat fluxes are emitted from the ocean to the cyclone, because of the high-speed winds. This process reaches a maximum near the radius of maximum wind (RMW), and then decreases gradually outwards. With consideration of typhoon-induced SST cooling, the total heat flux in CEX is much smaller than that in UEX in the inner-core region, and less heat flux is provided to the vortex by the underlying ocean. There is no vortex-shaped symmetrical distribution of the total heat flux and almost no similarity to the distribution of wind (see Fig. 6b).

The time-radius cross section of azimuthally averaged total heat fluxes on D02 for CEX and UEX are compared in Fig. 7a and Fig. 7c. The total heat flux in UEX reaches the maximum when the radius is in the range of 60–90 km. Especially after 1200 UTC 15 May, the total heat flux is over 2000 W m^{-2} in this area. The heat flux outside of the inner-core region is generally in the range of 1200–1500 W m^{-2}, and has little change with time. In the early part of the integration, the heat flux in CEX is similar to that of UEX. After 1800 UTC 14 May, the heat flux in the inner-core region of the typhoon is much less than that simulated by UEX.

It is known that SST cooling reduces the sensible and latent heat fluxes from ocean to the vortex, especially in the inner-core region. A reduction of the surface heat flux diminishes the moist static energy. In an approximate steady-state theory for a hurricane that assumes neutrality to slantwise convection throughout the vortex, Emanuel (1986) derived a simple linear relationship between the differences in the equivalent potential temperature $\Delta\theta_e$ and the sea level pressure

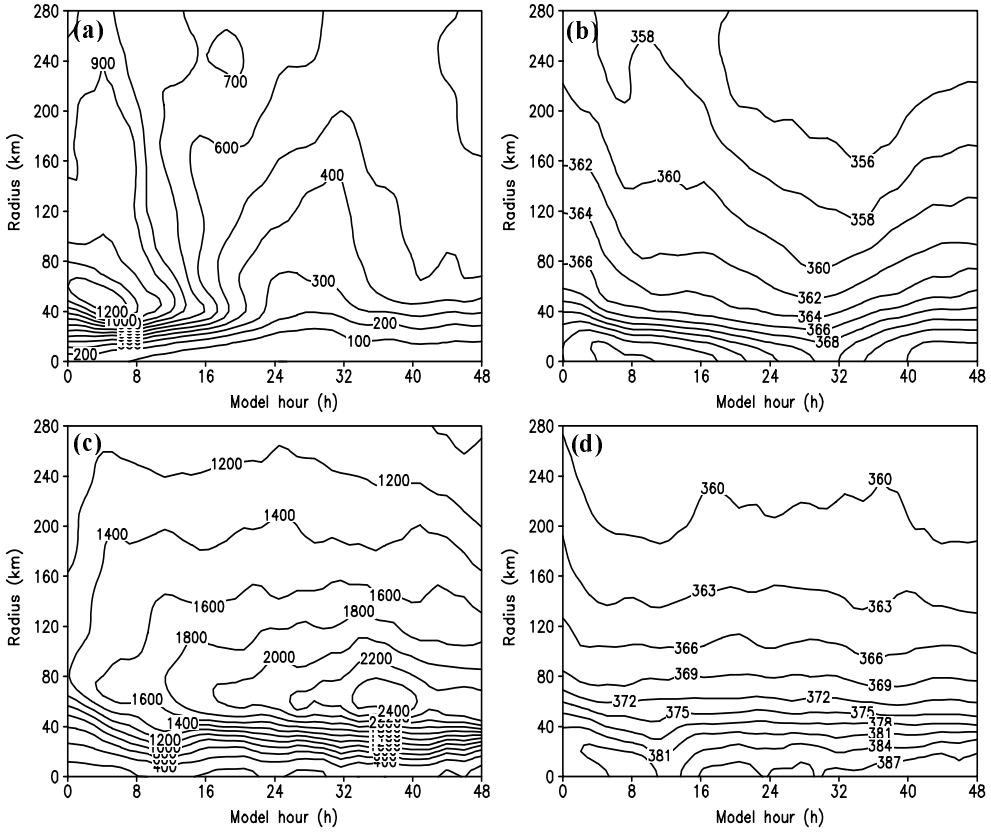

Fig. 7. The time-radius cross section of azimuthally averaged fields over D02 for (a, b) CEX and (c, d) UEX. (a), (c): total heat fluxes (Units: W m^{-2}) ; (b), (d): equivalent potential temperature (Units: K).

ΔP between the storm center and the outer storm periphery: $\Delta P = -(3.3)\Delta\theta_e$. Bender and Ginis (2000) indicated some variability in the ratio $-\Delta P/\Delta\theta_e$ with values lying between 3.1 and 4.2. However, the two studies highlighted the relationship between vortex intensity as measured by ΔP and the elevation of θ_e near the vortex center. Therefore, it is necessary to examine the effects of ocean coupling on the distributions of boundary layer moist static energy in CEX and UEX. Taking the lowest model level (σ=0.995, ~36 m height) in the models as an example, Figs. 7b and 7d show that there is a relatively big difference in θ_e in the inner-core region of the typhoon between CEX and UEX, whereas outside of the inner-core region the difference is relatively small. In the inner-core region, θ_e decreases rapidly outwards. Comparing CEX and UEX at 0900 UTC 15 May, over a distance of 111 km from the center, θ_e increases by 14 K and 22 K, respectively. UEX has the larger radial gradient of moist static energy, and a stronger radial gradient of moist static energy is associated with a more intense vortex (Zhu et al., 2004). In light of the temporal development of θ_e, there is a relatively big change in θ_e in the inner-core regions of the two typhoons simulated by CEX and UEX.

To quantify the impact of the variation in SSTs within the inner core on the typhoon intensity, Fig. 8 shows the time series of the area-averaged SSTs and total heat fluxes within the inner core for the two experiments, following the typhoon's movement. One can see that the SST differences within the inner core are small during the first 12 h, and the time series of the area-averaged SST in CEX shows a steady drop from 1800 UTC 12 May to 0900 UTC 15 May. At 0900 UTC 15 May, SST is 26.15°C, which is 5.15°C lower than that in UEX. Thereafter it experiences little increase. Because it doesn't incorporate the typhoon-induced SST cooling, the area-averaged SST in UEX shows little change from 0600 UTC 13 May to 1500 UTC 16 May. On average, the SST in CEX is 2.17°C colder than that in UEX (see Table 1), thus the 46-hPa central pressure difference between CEX and UEX yields a 21.3 hPa deepening with a 1°C increase in SST within the inner core. The deepening rate of 21.3 hPa per degree is close to the deepening rates that Zhu and Zhang (2006) and Chan et al. (2001) obtained.

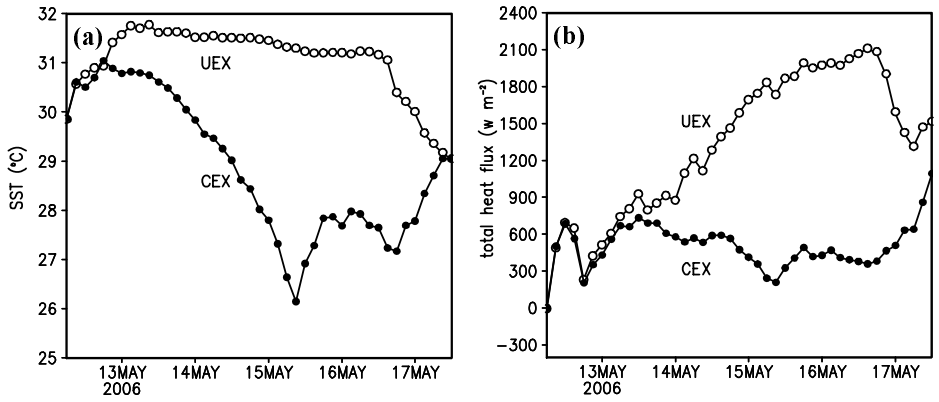

Fig. 8. Time series of (a) the area-averaged SST, (b) total heat flux in the inner-core region for CEX and UEX.

Table 1. Area-averaged sensible heat flux, latent heat flux, total heat flux, and SST in inner-core region from 0600 UTC 12 May to 1200 UTC 17 May for CEX and UEX.

	Latent heat flux (W m^{-2})	Sensible heat flux (W m^{-2})	Total heat flux (W m^{-2})	SST (°C)
CEX	508.45	16.97	525.42	28.89
UEX	1084.20	142.88	1227.08	31.05

Schade and Emanuel, 1999 defined the SST feedback factor $F_{\rm SST}$ to quantitatively measure the ocean's interactive effects on a hurricane's intensity:

$$F_{\rm SST} = \frac{\Delta p}{\Delta p|_{\rm SST}} - 1$$

where Δp is the difference between the background surface pressure far away from the storm and the minimum central pressure in the eye. Here, Δp serves as a measure of storm intensity. The subscript SST refers to the pressure depression that occurs with a fixed sea surface temperature, that is, without any feedback. The factor $F_{\rm SST}$ is always negative because a reduction of the SST due to the storm diminishes the storm's intensity. Therefore $F_{\rm SST}$ must be in the range $[-1, 0]$. In this study, for CEX, $\Delta p = 54$ hPa and for UEX, $\Delta p|_{\rm SST}$=100 hPa, Therefore $F_{\rm SST} = -0.46$, which means that the typhoon-induced SST cooling can reduce the typhoon intensity by 46%. This result is similar to the 50% intensity change shown by Schade and Emanuel (1999) and 47% intensity change shown by Zhu and Zhang (2006).

For CEX, the time series of area-averaged total heat flux within the inner core shows strong resemblance to the SST variation. The total heat flux reaches its lowest value of 208.04 W m^{-2} at 0900 UTC 15 May when the SST is lowest. On average, the total heat flux in CEX is 701.66 W m^{-2} lower than that in UEX (see Table 1), which is a reduction of 57.2%. The rate of the total surface heat fluxes is 323.35 W m^{-2} per degree change, which is similar to the typical observed flux anomalies of 50 W m^{-2} with 0.2°C SST changes found by Cayan (1992). In addition, as shown in Table 1, the latent heat flux is dominant over sensible heat flux during the whole integration stage for both CEX and UEX. Thus the latent heat flux makes much more significant contributions to the total energy source of the typhoon, which has been shown to be a dominant force in the development of mesoscale structures in the marine atmospheric boundary layer (MABL) (Warner et al., 1990).

5. Summary and conclusions

It is well accepted that the upper ocean can have a significant impact on modifying typhoon intensity and structure. However, exactly how and to what extent variations in upper-ocean thermal structure directly impact typhoon intensity and structure is still not well understood. In this paper, a mesoscale coupled air-sea model is developed based on the non-hydrostatic mesoscale model MM5 and the regional ocean model POM. The air-sea interactions during the life cycle of a typhoon and the quantifiable effects of typhoon-induced (SST) cooling on typhoon intensity are investigated.

In this study, two experiments are performed, one using the coupled model (denoted CEX) and the other using only MM5 (denoted UEX), with a fixed SST field so that the typhoon-induced cooling is ignored. In the absence of SST cooling, UEX produces a much stronger typhoon than CEX, with a value 46 hPa

deeper in central pressure than that in CEX. Moreover UEX fails to reproduce the weakening stage of Typhoon Chanchu from 1200 UTC 15 May to 1800 UTC 16 May. On average, the SST in CEX is 2.17°C colder than that in UEX. Thus the 46 hPa central pressure difference between CEX and UEX yields a 21.3 hPa deepening with a 1°C increase in SST within the inner core. The deepening rate of 21.3 hPa per degree is close to the deepening rates that Zhu and Zhang (2006) and Chan et al. (2001) obtained. The typhoon-induced SST cooling reduces the sensible and latent heat fluxes from the ocean to the vortex, especially in the inner-core region. In this study, the average total heat fluxes in the inner-core region of the typhoon decreases by 57.2%, whereas typhoon intensity weakens by 46%, correspondingly.

The simulation results in CEX show that the SST cooling makes the distributions of wind and total heat flux around the typhoon center more asymmetric. Thus we may state that air-sea interactions make some contributions to the formation of the typhoon asymmetry. The impact of SST cooling on typhoon structure is under study and will be given in a forthcoming paper.

Acknowledgements. This study was jointly supported by the National Natural Science Foundation of China (Grant No. 40675065) and National Key Basic Research Development Program (Grant Nos. 2007CB411805 and 2006CB403600) The authors thank the two anonymous reviewers for their sound criticism and valuable comments, which led to the substantial improvement of this paper.

REFERENCES

Bao, S., L. Xie, and S. Raman, 2004: A numerical study of a TOGA-COARE squall-line using a coupled mesoscale atmosphere-ocean model. *Adv. Atmos. Sci.*, **21**(5), 708–716.

Bender, M. A., and I. Ginis, 2000: Real-case simulations of hurricane-ocean interaction using a high-resolution coupled model: effects on hurricane intensity. *Mon. Wea. Rev.*, **128**, 917–945.

Cayan, D. R., 1992: Latent and sensible heat flux anomalies over the northern oceans: Driving the sea surface temperature. *J. Phys. Oceanogr.*, **22**, 859–881.

Chan, J. C. L., Y. Duan, and L. K. Shay, 2001: Tropical cyclone intensity change from a simple ocean-atmosphere coupled model. *J. Atmos. Sci.*, **58**, 154–172.

Chang, S. W., and R. A. Anthes, 1978: Numerical simulation of ocean's nonlinear baroclinic response to translating hurricanes. *J. Phys. Oceanogr.*, **8**, 468–480.

Cione, J. J., and E. W. Uhlhorn, 2003: Sea surface temperature variability in hurricanes: implications with respect to intensity change. *Mon. Wea. Rev.*, **131**, 1783–1795.

Davis, C. A., and L. F. Bosart, 2001: Numerical simulations of the genesis of hurricane Diana (1984). Part I: Control Simulation. *Mon. Wea. Rev.*, **129**, 1859–1881.

Elsberry, R. L., T. Fraim, and R. Trapnell, 1976: A mixed layer model of the ocean thermal response to hurricane. *J. Geophys. Res.*, **81**(C6), 1153–1162.

Emanuel, K. A., 1986: An air-sea interaction theory for tropical cyclones, Part I: Steady-state maintenance. *J. Atmos. Sci.*, **43**, 585–604.

Emanuel, K. A., 1991: The theory of hurricanes. *Annual Review of Fluid Mechanics*, **23**, 179–196.

Falkovich, A. I., A. P. Khain, and I. Ginis, 1995: Motion and evolution of binary tropical cyclones in a coupled atmosphere-ocean numerical model. *Mon. Wea. Rev.*, **123**, 1345–1363.

Holland, G. J., 1997: The maximum potential intensity of tropical cyclones. *J. Atmos. Sci.*, **54**, 2519–2541.

Huang, L. W., G. X. Wu, and R. C. Yu, 2005: The effects of mesoscale air-sea interaction on heavy rain in two typhoon processes. *Acta Meteorologica Sinica*, **63**(4), 455–467. (in Chinese)

Khain, A. P., and I. D. Ginis, 1991: The mutual response of a moving tropical cyclone and the ocean. *Beitr. Phys. Atmos.*, **64**, 125–142.

Price, J. F., 1981: Upper ocean response to a typhoon. *J. Phys. Oceanogr.*, **11**, 153–175.

Price, J. F., T. B. Sanford, and G. Z. Forristall, 1994: Forced stage response to a moving hurricane. *J. Phys. Oceanogr.*, **24**, 233–260.

Ren, X., and W. Perrie, 2006: Air-sea interaction of typhoon Sinlaku (2002) simulated by the Canadian MC2 model. *Adv. Atmos. Sci.*, **23**(4), 521–530, doi: 10.1007/s00376-006-0521-4.

Sakaida, F., H. Kawamura, and Y. Toba, 1998: Sea surface cooling caused by typhoons in the Tohuku area in August 1989. *J. Geophys. Res.*, **103**(C1), 1053–1065.

Schade, L. R., and K. A. Emanuel, 1999: The ocean's effect on the intensity of tropical cyclones: results from a simple coupled atmosphere-ocean model. *J. Atmos. Sci.*, **56**, 642–651.

Shay, L. K., P. G. Black, A. J. Mariano, J. D. Hawkins, and R. L. Elsberry, 1992: Upper ocean response to hurricane Gilbert. *J. Geophys. Res.*, **97**(C12), 20227–20248.

Shay, L. K., J. G. Gustavo, and P. G. Black, 2000: Effects of a warm oceanic feature on Hurricane Opal. *Mon. Wea. Rev.*, **128**, 1366–1383.

Sheng, J., X.-M. Zhai, and R. J. Greatbatch, 2006: Numerical study of the storm-induced circulation on the Scotian Shelf during Hurricane Juan using a nested-grid ocean model. *Progress in Oceanography*, **70**, 233–254.

Sutyrin, G. G., and A. P. Khain, 1979: Interaction of ocean and the atmosphere in the area of moving tropical cyclone. *Dokl. Akad. Aauk USSR*, **249**, 467–470.

Sutyrin, G. G., and A. P. Khain, 1984: On the effect of air-ocean interaction on the intensity of a moving tropical cyclone. *Atmospheric and Oceanic Physics*, **20**, 787–794.

Wada, A., 2005: Numerical simulations of sea surface cooling by a mixed layer model during the passage of typhoon Rex. *J. Phys. Oceanogr.*, **61**, 41–57.

Warner, T. T., M. N. Lakhtakia, J. D. Doyle, and R. A. Pearson, 1990: Marine atmospheric boundary layer circulations forced by Gulf Stream sea surface temperature gradients. *Mon. Wea. Rev.*, **118**, 309–323.

Weatherford, C. L., and W. M. Gray, 1988: Typhoon structure as revealed by aircraft reconnaissance. Part I: Data analysis and climatology. *Mon. Wea. Rev.*, **116**, 1032–1043.

Zhang, Y. C., and Y. F. Qian, 1999: Numerical simulation of the regional ocean circulation in the coastal area of China. *Adv. Atmos. Sci.*, **16**(3), 443–450.

Zhu, H., W. Ulrich, and R. K. Smith, 2004: Ocean effects on tropical cyclone intensification and inner-core asymmetries. *J. Atmos. Sci.*, **61**, 1245–1258.

Zhu, T., and D.-L. Zhang, 2006: The impact of the storm-induced SST cooling on hurricane intensity. *Adv. Atmos. Sci.*, **23**(1), 14–22.